Inorg. Chem. **2006**, *45*, 1646–1655

Structure of Organic and Metal–Organic Networks Based on a Bifunctional *m*-Terphenyl Carboxylic Acid

Diane A. Dickie,[†] Gabriele Schatte,[‡] Michael C. Jennings,[§] Hilary A. Jenkins,[||] Sarah Y. L. Khoo,[†] and Jason A. C. Clyburne*,[†]

Department of Chemistry, Simon Fraser University, Burnaby, British Columbia V5A 1S6, Canada; Saskatchewan Structural Sciences Centre, University of Saskatchewan, Saskatoon, Saskatchewan S7N 5C9, Canada; Department of Chemistry, University of Western Ontario, London, Ontario N6A 5B7, Canada; Department of Chemistry, Saint Mary's University, Halifax, Nova Scotia B3H 3C3, Canada

Received September 30, 2005

A series of metal-organic frameworks (MOFs) based upon the ligand 2,6-diphenyl-1,4-dibenzoic acid $[Ph_2C_6H_2(CO_2H)_2]_\infty$ have been prepared and characterized by X-ray crystallography. The networks exhibit a variety of topologies and coordination modes at the metal center. The reaction of the ligand with cobalt(II) nitrate or zinc(II) nitrate in methanol/pyridine results in the formation of isostructural 1-D chains $[(Ph_2C_6H_2(CO_2)_2)M(py)_2(MeOH)]_\infty$, where M = Zn, Co; however, in the presence of ethanol and triethylamine, $Zn(NO_3)_2$ reacts to form a 2-D clay-like network, $[(Ph_2C_6H_2(CO_2)_2)Zn(EtOH)_2]_\infty$. 2-D networks are also formed in similar reactions with copper(II) nitrate or silver(I) nitrate to give $[(Ph_2C_6H_2(CO_2)(CO_2H))_2Cu(py)_2]_\infty$, $[(Ph_2C_6H_2(CO_2)CO_2H))_2Cu(py)_4\cdot 2H_2O]_\infty$, and $[(Ph_2C_6H_2(CO_2)_2)Ag_2]_\infty$, respectively. The hydrogen-bonded chains formed by the ligand alone and with 4,4′-dipyridyl are also described.

Introduction

Metal–organic frameworks (MOFs) are hybrid materials composed of metal atoms or clusters with a well-defined coordination geometry coordinated to nitrogen or oxygen donors within a variety of functionalized organic spacer ligands. This combination ideally leads to the formation of a rigid, crystalline, two- or three-dimensional network analogous to inorganic zeolites. While the ability of MOFs to form rare or unique supramolecular structures makes them interesting from a fundamental standpoint, it is primarily the ability to design and tune various properties of the MOFs that has driven their development for applied chemistry. MOFs are being used in laboratory settings for applications including catalysis[1] and nonlinear optic (NLO) materials.[2] A recent article in Chemical and Engineering News highlighted the potential for MOFs in hydrogen storage,[3] and other gas sorption behavior is being studied.[4] MOFs have also been shown to exhibit interesting magnetic[5] and luminescent[6] behavior. Several of these properties, particu-

* To whom correspondence should be addressed. E-mail: clyburne@sfu.ca.
[†] Simon Fraser University.
[‡] University of Saskatchewan.
[§] University of Western Ontario.
[||] Saint Mary's University.

(1) (a) Wu, C.-D.; Hu, A.; Zhang, L.; Lin, W. *J. Am. Chem. Soc.* **2005**, *127*, 8940–8941. (b) Kesanli, B.; Lin, W. *Coord. Chem. Rev.* **2003**, *246*, 305–326. (c) Fujita, M.; Kwon, Y. J.; Washizu, S.; Ogura, K. *J. Am. Chem. Soc.* **1994**, *116*, 1151–1152.
(2) (a) Wang, Y.-T.; Fan, H.-H.; Wang, H.-Z.; Chen, X.-M. *Inorg. Chem.* **2005**, *44*, 4148–4150. (b) Han, L.; Hong, M.; Wang, R.; Luo, J.; Lin, Z.; Yuan, D. *Chem. Commun.* **2003**, 2580–2581. (c) Evans, O. R.; Lin, W. *Acc. Chem. Res.* **2002**, *35*, 511–522.
(3) (a) Jacoby, M. *Chem. Eng. News* **2005**, *83*, 42–47. (b) Rowsell, J. L. C.; Yaghi, O. M. *Angew. Chem., Int. Ed.* **2005**, *44*, 4670–4679.
(4) (a) Sudik, A. C.; Millward, A. R.; Ockwig, N. W.; Côté, A. P.; Kim, J.; Yaghi, O. M. *J. Am. Chem. Soc.* **2005**, *127*, 7110–7118. (b) Rowsell, J. L. C.; Millward, A. R.; Park, K. S.; Yaghi, O. M. *J. Am. Chem. Soc.* **2004**, *126*, 5666–5667. (c) Kitaura, R.; Seki, K.; Akiyama, G.; Kitagawa, S. *Angew. Chem., Int. Ed.* **2003**, *42*, 428–431. (d) Eddaoudi, M.; Kim, J.; Rosi, N.; Vodak, D.; Wachter, J.; O'Keeffe, M.; Yaghi, O. M. *Science* **2002**, *295*, 469–472.
(5) (a) Tynan, E.; Jensen, P.; Kelly, N. R.; Kruger, P. E.; Lees, A. C.; Moubaraki, B.; Murray, K. S. *Dalton Trans.* **2004**, 3440–3447. (b) Mao, H.; Zhang, C.; Li, G.; Zhang, H.; Hou, H.; Li, L.; Wu, Q.; Zhu, Y.; Wang, E. *Dalton Trans.* **2004**, 3918–3925. (c) Moulton, B.; Lu, J.; Hajndl, R.; Hariharan, S.; Zaworotko, M. J. *Angew. Chem., Int. Ed.* **2002**, *41*, 2821–2824. (d) Cao, R.; Shi, Q.; Sun, D.; Hong, M.; Bi, W.; Zhao, Y. *Inorg. Chem.* **2002**, *41*, 6161–6168. (e) Sanselme, M.; Grenèche, J. M.; Riou-Cavellec, M.; Férey, G. *Chem. Commun.* **2002**, 2172–2173.
(6) (a) Lee, E. Y.; Jang, S. Y.; Suh, M. P. *J. Am. Chem. Soc.* **2005**, *127*, 6374–6381. (b) Zhao, B.; Chen, X.-Y.; Cheng, P.; Liao, D.-Z.; Yan, S.-P.; Jiang, Z.-H. *J. Am. Chem. Soc.* **2004**, *126*, 15394–15395. (c) Ma, A.-Q.; Zhu, L.-G. *Trans. Met. Chem.* **2004**, *29*, 329–331.

10.1021/ic051690g CCC: $33.50
Published on Web 01/13/2006

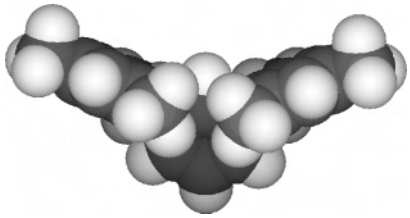

Figure 1. Space-filling model of 2,6-bis(2,4,6-trimethylphenyl)benzene. Note the bowl-shaped cavity of the *m*-terphenyl.

larly magnetism and NLO behavior, are also seen in one-dimensional (1-D) metal-organic chains, and these types of structure are also studied as molecular wires.[7]

Much research to date has focused on controlling pore size of the MOFs, but a significant emphasis has also been placed on controlling the environment around the metal center. Both catalysis and gas sorption, for example, can be altered or improved when the metal has a vacant coordination site to which the substrate can be bound.[8] This is often difficult to achieve because of the inherent reactivity of most metals. The variety and flexibility of coordination modes available in carboxylate ligands can often be exploited to open vacant coordination sites in molecular materials, but in extended networks, the carboxylate is often an important structural component and any change in coordination can have an adverse effect on the integrity of the network.

One class of ligand that truly stands out for its ability to protect low-coordinate metal sites is the *m*-terphenyl ligand.[9] These molecules, defined as a phenyl ring with at least two aryl substituents meta to one another off the central ring, provide a hydrophobic bowl-shaped pocket (Figure 1) in which a metal is sterically protected from aggregation but still available for reaction with small molecules. The steric demands of the ligand can be easily fine-tuned by varying the aryl substituents, while the coordination can be adjusted by altering the functional group through which the metal is bound.

m-Terphenyl ligands have been used extensively for the stabilization of unusual coordination environments (e.g., multiple bonds) in both main group elements and transition metals.[10] They are also used for applications including catalysis[11] and enzyme mimicry[12] and have recently been incorporated into functional materials including conjugated polymers[13] and self-assembled monolayers.[14] *m*-Terphenyl ligands, therefore, seemed to be ideal candidates for incorporation into MOFs. Herein, we report the synthesis and structural characterization of a series of metal−organic 1-D chains and two-dimensional (2-D) networks featuring a bifunctional carboxylic acid *m*-terphenyl backbone,[15] 2,6-diphenyl-1,4-dibenzoic acid (**1H$_2$**). Also described in this paper is a purely organic hydrogen-bonded chain (**2**) made of alternating molecules of 4,4′-dipyridyl with **1H$_2$**. The MOFs, based on zinc(II) (**3**, **8**), cobalt(II) (**4**), copper(II) (**5**, **6**), and silver(I) (**7**), exhibit a variety of carboxylate coordination modes and a corresponding assortment of structural topologies. In all of the networks except **7**, the carboxylate ligand also engages in significant hydrogen bonding with solvent molecules. These metals were chosen as a representative cross-section of the metals commonly used to prepare MOFs with the properties described above.

Experimental Section

General. NMR spectra were recorded on a Bruker AMX 400 or a Varian AS 500 spectrometer in 5 mm quartz tubes. ^{1}H and ^{13}C{^{1}H} chemical shifts are reported in parts per million (ppm) downfield from tetramethylsilane (TMS) and are calibrated to the residual signal of the solvent. Infrared spectra were obtained using a Bomem MB spectrometer with the percent transmittance values reported in cm^{-1}. Melting points were measured using a Mel-Temp apparatus and are uncorrected. Elemental analyses were obtained on a Carlo Erba Model 1106 CHN analyzer.

Synthesis. (1H$_2$) 2,6-Diphenyl-1,4-dibenzoic Acid. Potassium permanganate (4.11 g, 26.0 mmol) and sodium carbonate (3.00 g, 28.3 mmol) were dissolved in 100 mL of water. To this solution was added 4-methyl-2,6-diphenylbenzoic acid (3.00 g, 10.4 mmol) and Tide laundry detergent[16] (0.30 g). The mixture was heated to reflux for 2 h then cooled to room temperature. Sodium bisulfite was added in small solid portions until the solution was colorless, and then the brown precipitate was removed by filtration through Celite. The solution was cooled to 0 °C, and concentrated HCl (12 mL) was added dropwise, resulting in the formation of a white precipitate. The mixture was extracted with Et_2O and dried with $MgSO_4$. Slow evaporation of the solvent in air gave colorless crystals. Yield = 2.59 g (82%). mp = 325−327 °C. ^{1}H NMR (DMSO-d_6, 499.770 MHz) δ 13.1 (br s, O*H*), 7.87 (s, 2H), 7.39−7.49 (m, 10H). ^{13}C{^{1}H} (DMSO-d_6, 125.680 MHz) δ 170.2, 167.1, 140.0, 139.9, 138.2, 133.5, 131.9, 130.1, 129.9, 129.2, 129.0, 128.6. IR (Nujol) ν 1692 (s), 1568 (w), 1496 (w), 1337 (w), 1267 (m), 1098 (w), 787 (w), 700 (w). Anal. Calcd for $C_{20}H_{14}O_4$: C, 75.46; H, 4.43. Found: C, 75.57; H, 4.48.

(2) 1H$_2$·4,4′-Bipy. 4,4′-Dipyridyl (0.12 g, 0.78 mmol) was dissolved in 5 mL of ethanol and added dropwise to a solution of

(7) (a) Zaman, M. B.; Udachin, K.; Ripmeester, J. A.; Smith, M. D.; zur Loye, H. C. *Inorg. Chem.* **2005**, *44*, 5047−5059. (b) Plater, M. J.; Foreman, M. R. S. J.; Slawin, A. M. Z. *Inorg. Chim. Acta* **2000**, *303*, 132−136, and references therein.

(8) (a) Chen, B.; Ockwig, N. W.; Millward, A. R.; Contreras, D. S.; Yaghi, O. M. *Angew. Chem., Int. Ed.* **2005**, *44*, 4745−4749. (b) Chen, B.; Eddaoudi, M.; Reineke, T. M.; Kampf, J. W.; O'Keeffe, M.; Yaghi, O. M. *J. Am. Chem. Soc.* **2000**, *122*, 11559−11560.

(9) For reviews of *m*-terphenyl chemistry, see: (a) Twamley, B.; Haubrich, S. T.; Power, P. P. *Adv. Organomet. Chem.* **1999**, *44*, 1. (b) Clyburne, J. A. C.; McMullen, N. *Coord. Chem. Rev.* **2000**, *210*, 73−99.

(10) (a) Power, P. P. *J. Organomet. Chem.* **2004**, *689*, 3904−3919. (b) Setaka, W.; Hirai, K.; Tomioka, H.; Sakamoto, K.; Kira, M. *J. Am. Chem. Soc.* **2004**, *126*, 2693−2697.

(11) (a) Dickie, D. A.; Jalali, H.; Samant, R. G.; Jennings, M. C.; Clyburne, J. A. C. *Can. J. Chem.* **2004**, *82*, 1346−1352. (b) Schmidt, J. A. R.; Arnold, J. *Organometallics* **2002**, *21*, 2306−2313.

(12) (a) Lee, D.; Hung, P.-L.; Spingler, B.; Lippard, S. J. *Inorg. Chem.* **2002**, *41*, 521−531. (b) Chavez, F. A.; Que, L., Jr.; Tolman, W. B. *Chem. Commun.* **2001**, 111−112.

(13) Smith, R. C.; Protasiewicz, J. D. *J. Am. Chem. Soc.* **2004**, *126*, 2268−2269.

(14) Dickie, D. A.; Chan, A. Y. C.; Jalali, H.; Jenkins, H. A.; Yu, H.-Z.; Clyburne, J. A. C. *Chem. Commun.* **2004**, 2432−2433.

(15) This ligand and complex **8** were previously reported in a communication. Dickie, D. A.; Jennings, M. C.; Jenkins, H. A.; Clyburne, J. A. C. *Inorg. Chem.* **2005**, *44*, 828−830.

(16) Addition of a surfactant improves the yield of this reaction by approximately 20%. Sodium dodecyl sulfate works very well; however commercial laundry detergents such as Tide work equally well and are often more readily available. This synthesis is based on the oxidation of toluene to benzoic acid in: Schoffstall, A. M.; Gaddis, B. A.; Druelinger, M. L. *Microscale and Miniscale Organic Chemistry Laboratory Experiments*, 2nd ed.; McGraw-Hill: Toronto, 2004.

Table 1. Crystallographic Data for Complexes of All Compounds

	1H$_2$	**2**	**3**	**4**	**5**	**6**	**7**	**8**
formula	$C_{20}H_{14}O_4$	$C_{30}H_{22}N_2O_4$	$C_{31}H_{26}N_2O_5Zn$	$C_{31}H_{26}CoN_2O_5$	$C_{50}H_{36}CuN_2O_8$	$C_{120}H_{100}Cu_2N_8O_{20}$	$C_{20}H_{12}Ag_2O_4$	$C_{24}H_{24}O_6Zn$
fw	318.31	474.50	571.91	565.47	856.35	2101.18	532.04	473.80
CCDC no.	266027	279136	279137	279138	279139	279140	279141	266026
T, K	173(2)	173(2)	173(2)	223(2)	173(2)	223(2)	150(2)	295(2)
color	colorless	colorless	colorless	pink	blue	blue	colorless	colorless
size	.10 × .10 × .20	.20 × .25 ×.25	.05 × .13 × .13	.04 × .28 × .34	.15 × .20 × .20	.06 × .25 × .40	.08 × .27 × .47	.20 × .22 × .28
cryst syst	tetragonal	monoclinic	monoclinic	monoclinic	orthorhombic	triclinic	monoclinic	triclinic
space group	$P4_12_12$	$P2_1/c$	$P2_1/n$	$P2_1/n$	$Pbca$	$P\bar{1}$	$C2/c$	$P\bar{1}$
a, Å	13.5640(3)	10.4550(2)	10.6080(2)	10.640(1)	17.2170(2)	9.3336(5)	17.334(1)	11.1000(3)
b, Å	13.5640(3)	13.3910(3)	14.9550(4)	15.018(2)	12.9640(3)	11.7460(6)	11.1485(9)	13.6800(6)
c, Å	17.0150(4)	19.0530(5)	16.4450(4)	16.425(2)	18.7630(4)	24.569(1)	9.4161(5)	15.7170(6)
α, deg	90	90	90	90	90	76.949(1)	90	98.866(2)
β, deg	90	116.6730(8)	90.676(1)	90.703(2)	90	86.176(1)	114.154(4)	90.857(2)
γ, deg	90	90	90	90	90	79.1960(10)	90	95.610(2)
V, Å	3130.4(1)	2383.61(9)	2608.7(1)	2624.5(6)	4187.9(1)	2576.6(2)	1660.4(2)	2345.6(1)
Z	8	4	4	4	4	1	4	4
D_{calc}, Mg·m^{-3}	1.351	1.322	1.456	1.431	1.358	1.354	2.128	1.342
μ, mm^{-1}	0.094	0.089	0.987	0.699	0.580	0.489	2.382	1.082
R1[a]	0.0396	0.0518	0.0463	0.0422	0.0426	0.0398	0.0330	0.0657
wR2[a]	0.0808	0.1190	0.0946	0.0970	0.0954	0.0777	0.0833	0.1806

[a] $R1 = [\sum||F_o| - |F_c||]/[\sum|F_o|]$ for $[F_o^2 > 2\sigma(F_o^2)]$; $wR2 = \{[\sum w(F_o^2 - F_c^2)^2]/[\sum w(F_o^2)^2]\}^{1/2}$ [all data].

1 (0.25 g, 0.78 mmol) in 5 mL of ethanol. Slow evaporation at room temperature over 3 days gave large, colorless plates. Yield: 0.27 g (73%). mp = 225 °C. ^{1}H NMR (DMSO-d_6, 400.136 MHz) δ 8.72 (d, J = 4.6 Hz, 4H), 7.87 (s, 2H), 7.83 (d, J = 4.7 Hz, 4H), 7.43−7.49 (m, 10H). IR (Nujol) ν 1704(s), 1599 (s), 1405 (m), 1283 (m), 1260 (s), 1214 (s), 1137 (w), 1057 (m), 1050 (m), 903 (w), 807 (s), 782 (s), 759 (s), 720 (m), 697(s), 628 (s). Anal. Calcd for $C_{30}H_{22}N_2O_4$: C, 75.94; H, 4.67; N, 5.90. Found: C, 75.62; H, 4.81; N, 5.71.

(3) 1·Zn·(py)$_2$·MeOH. 1 (0.25 g, 0.78 mmol) and $Zn(NO_3)_2\cdot 6H_2O$ (0.23 g, 0.78 mmol) were combined and dissolved in 8 mL of warm methanol. This solution was layered onto a solution of 0.1 mL of pyridine in 8 mL of benzene. After one week, the solution was carefully decanted from a white precipitate and allowed to slowly evaporate to give white crystals. Yield = 0.25 g (56%, based on Zn). mp > 350 °C. IR (Nujol) ν 3447 (br), 1693 (m), 1632 (w), 1606 (m), 1585 (m), 1573 (m), 1546 (m), 1447 (s), 1310 (m), 1153 (m), 1071 (m), 1042 (m), 913 (m), 796 (m), 753 (m), 698 (s). Anal. Calcd for $C_{31}H_{26}N_2O_5Zn$: C, 65.10; H, 4.58; N, 4.90. Found: C, 63.18; H, 4.61; N, 5.74 (discrepancy due to loss of solvent).

(4) 1·Co·(py)$_2$·MeOH. $Co(NO_3)_2\cdot 6H_2O$ (0.15 g, 0.51 mmol) was dissolved in 5 mL of methanol and added to a solution of **1** (0.35 g, 1.10 mmol) in 15 mL of methanol and 1 mL of pyridine. Slow solvent evaporation at room temperature gave dark pink crystals at the bottom of the reaction flask within hours. Yield = 0.25 g (87%, based on Co). mp > 320 °C (dec). IR (Nujol) ν 1601 (s), 1574 (s), 1538 (s), 1493 (m), 1486 (m), 1444 (vs), 1369 (vs), 1275 (w), 1216 (w), 1151 (w), 1070 (w), 1040 (s), 912 (m), 809 (m), 795 (s), 781 (m), 752 (s), 698 (vs). Anal. Calcd for $C_{31}H_{26}CoN_2O_5$: C, 65.84; H, 4.63; N, 4.95. Found: C, 65.52; H, 4.94; N, 4.99.

(5) (1H)$_2$·Cu·(py)$_2$. 1 (0.25 g, 0.78 mmol) and $Cu(NO_3)_2\cdot 2.5H_2O$ (0.18 g, 0.78 mmol) were dissolved in 8 mL of ethanol. This solution was layered onto a solution of 0.1 mL of pyridine in 8 mL of benzene. After 1 week, the solution was carefully decanted from a blue precipitate and allowed to slowly evaporate to give blue crystals. Yield = 0.26 g (39%, based on Cu). mp = 270−272 °C. IR (Nujol) ν 1867 (br), 1682 (vs), 1612 (m), 1580 (s), 1557 (s), 1455 (vs), 1331 (m), 1240 (s), 1219 (s), 1154 (m), 1106 (m), 1075 (m) 1049 (m), 912 (m), 822 (s), 695 (vs). Anal. Calcd for $C_{50}H_{36}N_2O_8Cu$: C, 70.13; H, 4.24; N, 3.27. Found: C, 70.05; H, 4.34; N, 3.34.

(6) (1H)$_2$·Cu·(py)$_4$·(H$_2$O)$_2$. $Cu(NO_3)_2\cdot 2.5H_2O$ (0.12 g, 0.51 mmol) was dissolved in 5 mL of methanol and added to a solution of **1** (0.35 g, 1.10 mmol) in 5 mL of methanol and 1 mL of pyridine. Slow solvent evaporation at room temperature gave dark blue crystals at the bottom of the reaction flask within hours. Yield = 0.33 g (62% based on Cu). mp = 93−98 °C (dec). IR (Nujol) ν 3464 (s), 3063 (w), 3024 (w), 1964 (br), 1693 (m), 1605 (s), 1581 (s), 1564 (s), 1557 (s), 1493 (s), 1448 (vs), 1337 (s), 1283 (s), 1269 (vs), 1235 (w), 1218 (w), 1154 (m), 1103 (w), 1068 (s), 1042 (m), 905 (m), 818 (s), 788 (w), 777 (s), 757 (vs), 720 (s), 698 (vs). Anal. Calcd for $C_{60}H_{50}CuN_4O_{10}$: C, 68.59; H, 4.80; N, 5.33. Found: C, 68.38; H, 4.80; 5.43.

(7) 1·Ag$_2$. Potassium 2,6-diphenyl-1,4-dibenzoate (10 mL, 0.1M in H_2O) was placed in a test tube, and 6 mL of a 2:1 MeOH/H_2O solution was carefully layered onto the potassium solution. Silver nitrate (0.17 g, 1.0 mmol) was dissolved in 8 mL of warm methanol and layered onto the mixed solvent. The test tube was kept in the dark for 1 week, and then the solution was decanted off to leave needlelike crystals. Yield = 0.04 g (7.5% based on Ag). mp > 350 °C. IR (Nujol) 1611 (w), 1583 (vs), 1544 (m), 1536 (m), 1509 (m), 1492 (s), 1318 (m), 1156 (m), 1073 (m), 1029 (m), 914 (w), 880 (m), 832 (s), 805 (m), 766 (m), 750 (s), 722 (m), 701 (vs). Elemental analysis was not performed due to low yield.

(8) 1·Zn·(EtOH)$_2$. $Zn(NO_3)_2\cdot 6H_2O$ (0.47 g, 1.57 mmol) was dissolved in 10 mL of ethanol and added to a solution of 2,6-diphenyl-1,4-dibenzoic acid (0.50 g, 1.57 mmol) in 10 mL of ethanol. Triethylamine (0.5 mL) was allowed to vapor diffuse into the reaction. After one week, colorless crystals were isolated. Yield = 0.26 g (35%), mp > 350 °C. IR (Nujol) 3367 (br), 1604 (s), 1557 (s), 1495 (w), 1318 (w), 1051 (m), 700 (m), 668 (w). Anal. Calcd for $C_{24}H_{24}O_6Zn$: C, 60.84; H, 5.11. Found: C, 59.36; H, 5.40 (discrepancy due to loss of solvent).

Crystallography. A single crystal was mounted on a glass fiber (**1**, **4**, **6**−**8**) or a nylon fiber of a mounted CryoLoop (**2**, **3**, **5**) and centered on either a Seimens 1K SMART/CCD diffractometer (**1**, **4**, **6**) or a Nonius KappaCCD diffractometer (**2**, **3**, **5**, **7**, **8**) using Mo Kα radiation. Data were collected at the temperatures noted in Table 1 and corrected for absorption, Lorentz, and polarization effects using either SADABS (**1**, **4**, **6**) or HKL2000 DENZO-SMN (SCALEPACK) (**2**, **3**, **5**, **7**, **8**) software packages. Direct methods and Fourier techniques were used to solve the crystal structures. Refinement was conducted by full-matrix least-squares method on

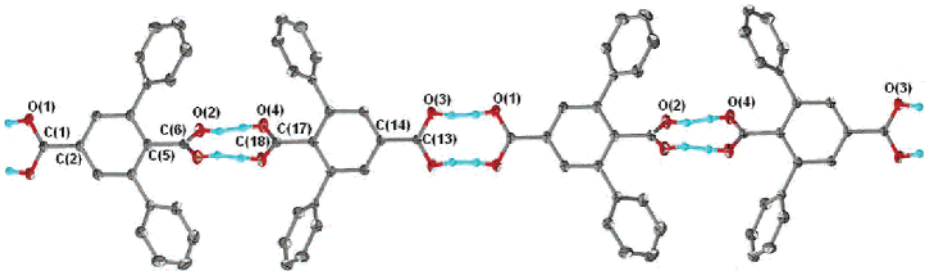

Figure 2. Hydrogen-bonded chain of $\mathbf{1H_2}$. Thermal ellipsoids are shown at 50% probability, and aryl hydrogen atoms have been removed for clarity.

F^2 using SHELXTL-PC V5.03 (**1**, **4**, **6**), SHELXL97-2 (**2**, **3**, **5**), or SHELXTL-NT V6.1 (**7**, **8**). All non-hydrogen atoms were refined with anisotropic displacement parameters except the ethanol molecules of **8**, which were refined with isotropic thermal parameters with the C−C (1.50 Å) and C−O (1.40 Å) distances being fixed. One ethanol molecule showed some disorder and was modeled as a 60/40 mixture of two molecules. The hydrogen atoms at the OH of the C(O)OH groups in **2** and **5** and the MeOH group in **3** were located in the Fourier difference map. Their atomic coordinates were allowed to refine, but the isotropic thermal parameter of these hydrogen atoms were fixed at 1.2× that of the preceding oxygen atom. All other hydrogen atoms were included at geometrically idealized positions and were not refined.

Results and Discussion

The oxidation of 4-methyl-2,6-diphenylbenzoic acid with potassium permanganate in water produces the bifunctional *m*-terphenyl 2,6-diphenyl-1,4-dibenzoic acid $\mathbf{1H_2}$ cleanly and in good yield. X-ray crystallographic studies (Table 1) revealed that this molecule forms infinite hydrogen-bonded chains in the solid state, alternating between two crystallographically distinct molecules (Figure 2). There is a plane of symmetry running along the center of each molecule, from C(1)−C(6) and C(13)−C(18). Consequently, the C−O bond lengths within each carboxylate are identical, with an average length of 1.264 Å. The intermolecular hydrogen bonding is strong and shows average [O···O] distances for neutral carboxylic acid chains,[17] at 2.648(3) Å for the less-hindered para carboxylate and 2.637(3) Å for the crowded, but more acidic, pocket carboxylate.

Studies have shown that the optimal conformation for unsubstituted aromatic carboxylic acids is coplanarity between the aromatic ring and the CO_2H fragments.[18] The presence of other favorable crystal packing interactions, such as hydrogen bonds, can have a significant impact on the twist angle since the energy required to rotate from 0° to 90° is only 20−40 kcal/mol.[18] Since the angle has also been shown to be dependent on the nature of ortho substituents,[19] it is not surprising that the steric demands imposed by the two phenyl substituents have an impact on the geometry of $\mathbf{1H_2}$. The pocket carboxylates twist significantly out of the plane of the central phenyl (46.88° and 68.45° in the two fragments), while the para-carboxylate is nearly coplanar (10.04° and 9.89°, respectively).[20] This results in a complimentary head-to-head alignment of the *m*-terphenyls, and essentially flat chains (Figure 3a) which are oriented antiparallel to neighboring chains and perpendicular to chains above and below (Figure 3b), in contrast to terephthalic acid which has all chains parallel.[21] Finally, although the central rings of the terphenyls in each chain are aligned in a face-to-face fashion, the bulk of the substituents pushes them too far apart (centroid···centroid = 4.414 Å) to be considered a π-stacking interaction.[22]

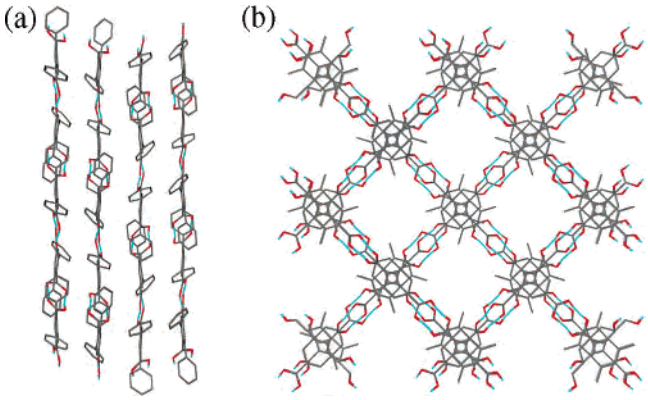

Figure 3. Packing diagrams of $\mathbf{1H_2}$ along the crystallographic *a* axis (a) and *c* axis (b). For clarity, only the ipso carbon ayoms of the flanking phenyls are shown in (b).

The reaction of $\mathbf{1H_2}$ with 4,4′-dipyridyl in ethanol gives a crystalline solid that contains the two molecules in a 1:1 ratio, as shown by solution ^{1}H NMR. X-ray crystallography showed an alternating hydrogen-bonded chain **2** (Figure 4) in the solid state. The plane of symmetry seen in $\mathbf{1H_2}$ is not present in complex **2**, resulting in distinct C═O and C−O bonds. The out-of-plane twisting of the para carboxylate is more pronounced, with an angle of 28.95°, compared to ca. 10°. The pocket carboxylate of **2** has a similar orientation (66.45°) to the more twisted of the two in the bifunctional *m*-terphenyl $\mathbf{1H_2}$ alone. The twist in the planes of the 4,4′-dipyridyl (13.29°) and the carboxylate combine to give the chains of **2** a wavy appearance, as opposed to the flat chains of $\mathbf{1H_2}$.

As in $\mathbf{1H_2}$, the hydrogen bond in the *m*-terphenyl pocket of **2** is slightly shorter, O(11)···N(51) = 2.631 Å, than in the para position, O(13)···N(41) = 2.641 Å. Both hydrogen

(17) Gilli, P.; Bertolasi, V.; Ferretti, V.; Gilli, G. *J. Am. Chem. Soc.* **1994**, *116*, 909−915.
(18) (a) Kaduk, J. A.; Golab, J. T. *Acta Crystallogr.* **1999**, *B55*, 85−94. (b) Kaduk, J. A. *Acta Crystallogr.* **2000**, *B56*, 474−485.
(19) Eddaoudi, M.; Kim, J.; O'Keeffe, M.; Yaghi, O. M. *J. Am. Chem. Soc.* **2002**, *124*, 376−377
(20) See Supporting Information for a table of twist angles for **1**−**8**.
(21) Śledź, M.; Janczak, J.; Kubiak, R. *J. Mol. Struct.* **2001**, *595*, 77−82 and references therein.
(22) Jorgensen, W. L.; Severance, D. L. *J. Am. Chem. Soc.* **1990**, *112*, 4768−4774.

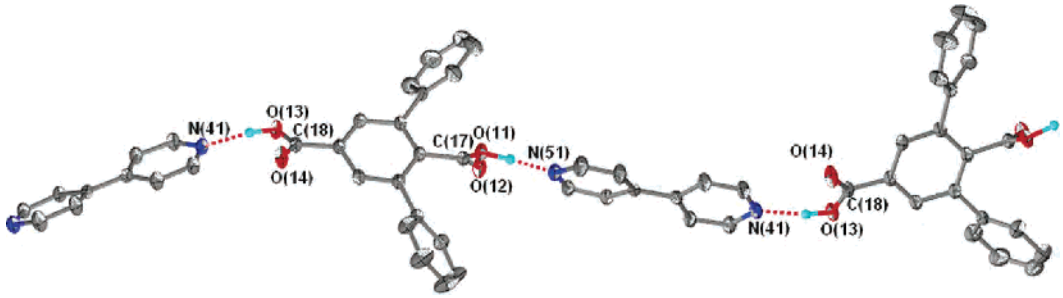

Figure 4. Hydrogen-bonded chain of **2**. Thermal ellipsoids are shown at 50% probability, and hydrogens, except for the O−H, have been removed for clarity.

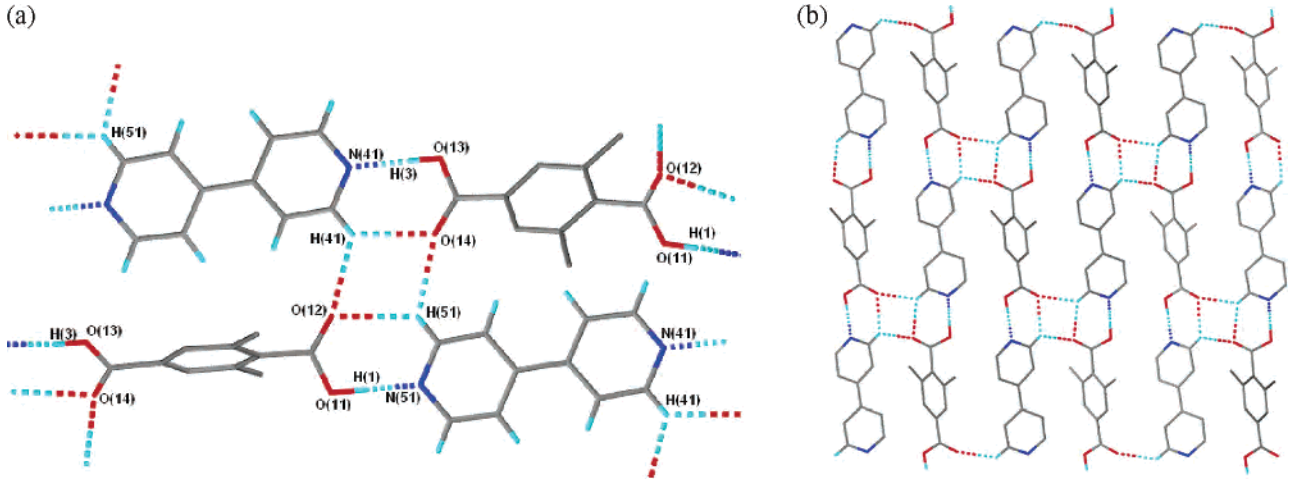

Figure 5. Strong [O−H···N] and weaker [C−H···O] interactions (a) in **2** produce a 2-D network (b) along the crystallographic *b* axis.

bonds are also very close to linear ([O−H···N] = 176.21° and 170.64° for the pocket and para, respectively) and within the ranges of typical carboxylic acid-bipyridine co-crystals.[23,24] In addition to the expected [O−H···N] hydrogen bonding, there is also extensive [C−H···O] hydrogen bonding.[25] By twisting significantly out of the plane of the central phenyl, the carboxylate is able to engage in the maximum number of interactions.[18] Each C═O acts as an acceptor to distinct C−H donors from two neighboring pyridyl fragments. The shortest bond for each carbonyl is to the hydrogen ortho to the pyridine nitrogen within the same chain. The distance for the pocket C═O is O(12)···H(51) = 2.588 Å, while the para C═O is again shorter at O(14)···H(41) = 2.399 Å, in the range of those reported between 4,4′-dipyridyl and bifunctional acids (2.26−2.57 Å).[23] The interactions with the ortho hydrogen of the pyridyl in the adjacent chain measure O(12)···H(41) = 2.599 Å in the pocket and O(14)···H(51) = 2.453 Å in the para position. When these interactions are taken into account, the 1-D chain becomes a 2-D network.

Attempts to use **2** or other combinations of **1H$_2$** and 4,4′-dipyridyl to prepare single-crystal MOFs have to date proven unsuccessful, giving insoluble precipitates. Instead, the reaction in the presence of excess pyridine of **1H$_2$** with either cobalt(II) nitrate or zinc(II) nitrate in methanol was performed. The pyridine completely deprotonates the two carboxylates to give 1-D chains **3** (M = Zn) and **4** (M = Co) with the general formula **1·M·(py)$_2$·MeOH** (Figure 6). Unlike the two organic chains, one methanol solvent molecule is coordinated to each metal ion, as seen in similar cobalt chains.[26,28] The metal is chelated by the para carboxylate and is also bound to two pyridine molecules that are oriented cis to one another, and the distorted octahedron of the metal coordination sphere is completed by the C−O of the pocket carboxylate, while the C═O forms a hydrogen bond to the methanolic O−H.

Table 2. Selected Bond Lengths (Å) of **3** and **4**[a]

bond	**3**, M = Zn	**4**, M = Co
M−O$_{(pocket)}$	2.037(2)	2.054(2)
M−O$_{1(para)}$	2.187(2)	2.151(2)
M−O$_{2(para)}$	2.2009(2)	2.183(2)
M−O$_{MeOH}$	2.177(2)	2.128(2)
M−N$_1$	2.092(3)	2.102(3)
M−N$_2$	2.162(2)	2.161(2)
O−H···O	d = 1.822, D = 2.626	d = 1.841, D = 2.625

[a] For the hydrogen bonds, d = [O···H] and D = [O···O] distances.

While the zinc (**3**) and cobalt (**4**) chains have the same connectivity, there are differences in the structural parameters (Table 2). The M−O$_{MeOH}$ bond and the M−O$_{para}$ bonds are all slightly longer in **3** than in **4**, but the pocket carboxylate has a shorter M−O bond. The pyridine M−N bonds are the same in both chains, within experimental error. The out-of-

(23) (a) Meiners, C.; Valiyaveettil, S.; Enkelmann, V.; Müllen, K. *J. Mater. Chem.* **1997**, *7*, 2367−2374. (b) Cowan, J. A.; Howard, J. A. K.; McIntyre, G. J.; Lo, S. M.-F.; Williams, I. D. *Acta Crystallogr.* **2003**, *B59*, 794−801.
(24) (a) Chatterjee, S.; Pedireddi, V. R.; Rao, C. N. R. *Tetrahedron Lett.* **1998**, *39*, 2843−2846. (b) Lough, A. J.; Wheatley, P. S.; Ferguson, G.; Glidewell, C. *Acta Crystallogr.* **2000**, *B56*, 261−272.
(25) (a) Desiraju, G. R. *Chem. Commun.* **2005**, 2995−3001. (b) Steiner, T. *Angew. Chem., Int. Ed.* **2002**, *41*, 48−76.

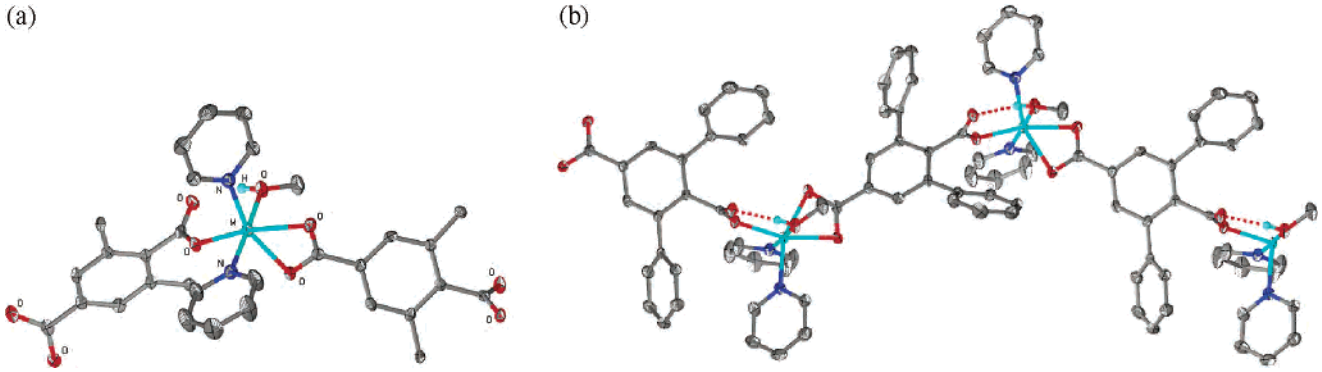

Figure 6. Molecular structure (a) and metal coordination polymer (b) of **4** (M═Co). Polymer **3** (M═Zn) is isostructural. Thermal ellipsoids are shown at 50% probability, and for clarity, all hydrogen atoms except the methanolic proton have been removed, as have the phenyls in (a).

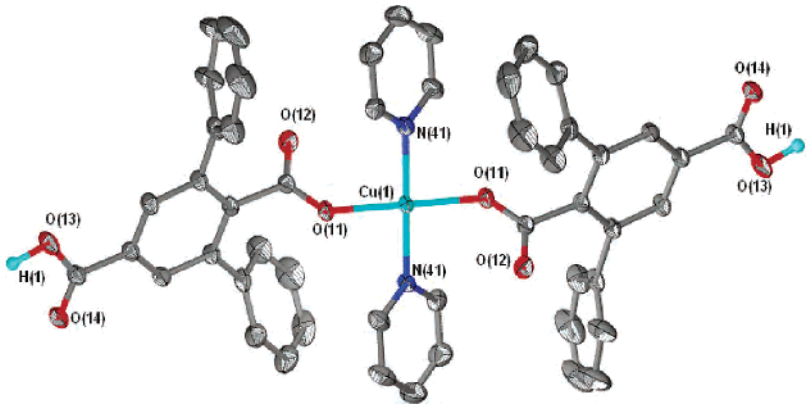

Figure 7. Molecular structure of **5**. Thermal ellipsoids are shown at 50% probability, and for clarity, only the O−H hydrogen is shown.

plane twist of the para carboxylate[20] was virtually identical in **2**, **3**, and **4** (ca. 28°) to maximize secondary [C−H···O] interactions between neighboring chains.[24]

The reaction of $\mathbf{1H_2}$ with copper(II) nitrate in ethanol with pyridine, although analogous to preparation of **3**, gives complex **5** with the significantly different formula $(\mathbf{1H})_2 \cdot Cu \cdot (py)_2$. No solvent is present, and only one of the two carboxylic acid moieties has been deprotonated, necessitating a 2:1 metal/ligand ratio in the neutral compound. Two pyridines are again present, but examination of the crystal structure showed that they are bound in trans conformation across a crystallographic mirror plane. The deprotonated pocket carboxylates are also trans and bound to the copper ions through a single oxygen, giving the metal square planar geometry (Figure 7) with O−Cu−N angles of 92.37(6)° and 87.63(6)°.

The Cu−O and Cu−N bond lengths of 1.9771(13) and 1.9948(18) Å, respectively, are significantly shorter than those seen in **3** and **4** and are also on the short end of the average reported for recent copper MOFs (Cu−O = 1.945−2.159 Å, Cu−N = 1.924−2.286 Å).[27,28] The difference of at least 0.05 Å for the M−O bond and 0.08 Å for the M−N bond may be caused by the increased demand for electron density from the solvent-free metal in **5**; it may also be due to the reduced steric hindrance around the four-coordinate copper compared to the six-coordinate zinc or cobalt in **3** and **4**. The C−O bonds in the pocket (1.252(2) and 1.246(2) Å, respectively) are delocalized, while those in the protonated para carboxylic acid can still be considered distinct single and double bonds (1.319(3) and 1.211(2) Å). In the pocket of the *m*-terphenyl ligand, the oxygen that is not bound to the metal is instead engaged in a very short[17] hydrogen bond (H···O = 1.466 Å, O···O = 2.495 Å, O−H···O = 159.71°) to the O−H of a neighboring para carboxylic acid. This brings the remaining C═O from the para group close enough to interact with the copper, transforming it from square planar to a Jahn−Teller[28] distorted octahedral geometry (Figure 8). This secondary Cu−O interaction measures 2.517 Å, nearly 0.5 Å less than the sum of the van der Waals radii of Cu(II) and O (2.92 Å), and is undoubtedly a significant interaction. The hydrogen bond and Cu−O interaction form a "figure eight" around the metal center, resulting in the formation of a 2-D network.

To demonstrate how sensitive MOF formation is to slight changes in reaction conditions, it is interesting to compare **5** with another complex formed by the reaction of 2 equiv of $\mathbf{1H_2}$ with copper(II) nitrate in methanol with excess pyridine. Slight variations in solvent and reaction stoichiometry gave a formula of $(\mathbf{1H})_2 \cdot Cu \cdot (py)_4 \cdot (H_2O)_2$ for complex **6**. As with **5**, compound **6** has a 2:1 ligand/metal ratio and

(26) Karanović, L.; Poleti, D.; Rogan, J.; Bogdanović, G. A.; Biré, A. S. *Acta Crystallogr.* **2002**, *C58*, m275−m279.
(27) (a) Wen, Y.-H.; Cheng, J.-K.; Feng, Y.-L.; Zhang, J.; Li, Z.-J.; Yao, Y.-G. *Inorg. Chim. Acta* **2005**, *358*, 3347−3354. (b) Zou, R.-Q.; Bu, X.-H.; Du, M.; Sui, Y.-X. *J. Mol. Struct.* **2004**, *707*, 11−15. (c) Ma, A.-Q.; Xu, D.-J.; Zhu, L.-G. *Acta Crystallogr.* **2003**, *E59*, m579−m581.
(28) Bourne, S. A.; Mondal, A.; Zaworotko, M. J. *Cryst. Eng.* **2001**, *4*, 25−36.

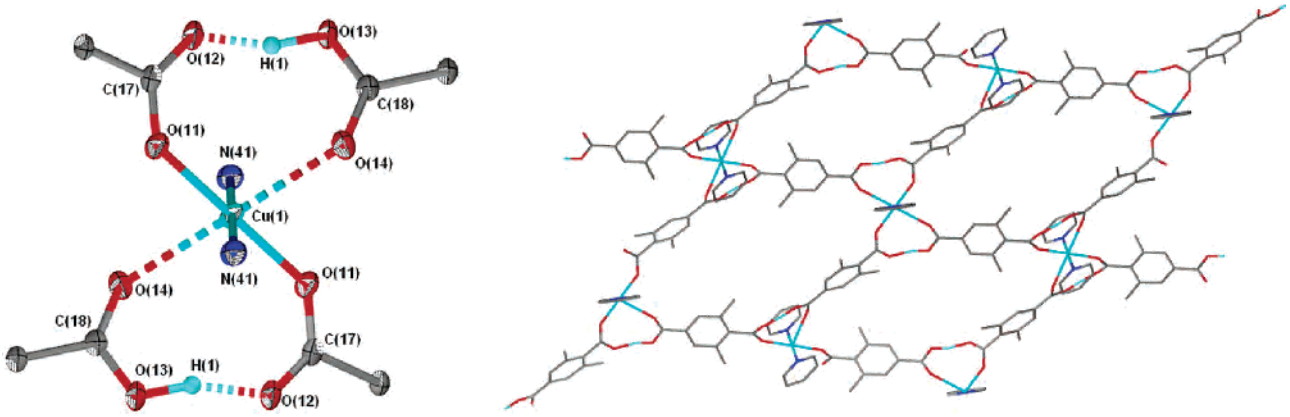

Figure 8. Extremely short [O−H···O] hydrogen bonds and long [Cu···O] interactions connecting a 2-D network. Phenyls removed for clarity.

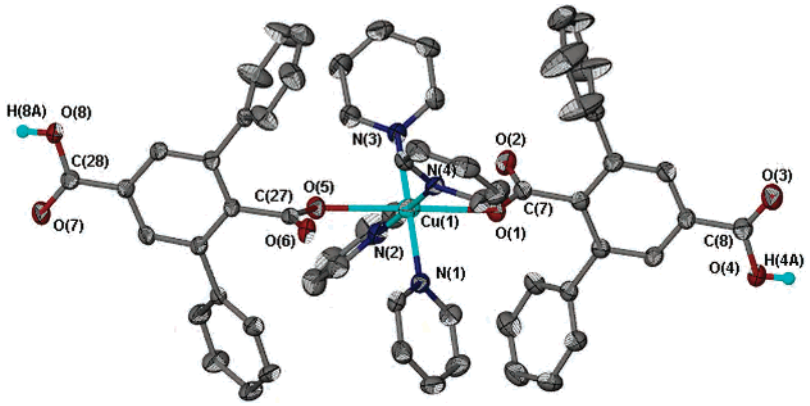

Figure 9. Structure of **6**. Thermal ellipsoids are shown at 50% probability, and for clarity, all hydrogens except the O−H have been removed. Two molecules of water are also not shown.

a singly deprotonated carboxylate, but it has incorporated twice as many pyridine molecules (Figure 9).

The four Cu−N bonds in **6** range from 2.025(2) to 2.040(2) Å, somewhat longer than those seen in **5**. The Cu−O bonds are also significantly longer, measuring 2.377(2) and 2.517(2) Å, compared to 1.9771(13) Å in **5**. In fact, the longer Cu(1)−O(5) bond is the same length as the secondary Cu−O in **5**. As with **5**, the C−O bond lengths in the pocket are indistinguishable, averaging 1.252 Å, indicating delocalization around the carboxylate fragment, despite the fact that the copper is clearly bound to only one of the two oxygens (nonbonded Cu(1)−O(2) = 3.802 Å and Cu(1)−O(6) = 3.945 Å). The protonated para position has distinct C═O and C−O bonds averaging 1.216 and 1.315 Å, respectively.

Given that the para and pocket carboxylates formed very strong hydrogen bonds to one another in **5**, a similar but perhaps weaker interaction might be expected in **6**. Examination of the extended structure, however, shows that it is in fact hydrogen bonding through the two waters of crystallization that give rise to a 2-D network made up of three distinct ring systems (Figure 10). The protonated para carboxylates of each *m*-terphenyl ligand bridge an oxygen and hydrogen from two water molecules to form the smallest ring. The remaining hydrogen atom from each water molecule forms a hydrogen bond to the unbound oxygen of the pocket carboxylate, completing and linking the two other rings. As shown in Table 3, the shortest hydrogen bonds are between water and the O−H of the para carboxylate, while the C═O of the para groups form the longest and the C−O of the pocket are intermediate. All of the bonds are of moderate to strong strength.[17] This network is further stabilized by extensive [C−H···O] hydrogen bonding be-

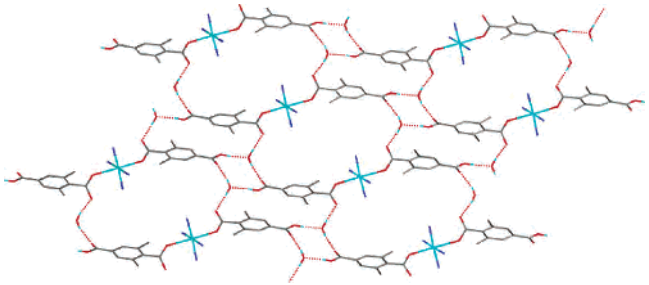

Figure 10. The carboxylate oxygens not bound to copper form hydrogen bonds with water to give this 2-D network. For clarity, only the ipso carbon atoms of the phenyls and the nitrogen of the pyridines are shown.

Table 3. [O-H···O] Hydrogen Bond Lengths and Angles in **6**[a]

	H···O (Å)	O···O (Å)	O−H···O (deg)
O(4)−H(4A)···O(9)#1	1.69	2.504(2)	168.3
O(8)−H(8A)···O(10)#2	1.69	2.518(2)	171.1
O(9)−H(9A)···O(3)#3	1.950(17)	2.796(2)	170(3)
O(9)−H(9B)···O(2)#4	1.787(16)	2.657(2)	177(3)
O(10)−H(7A)···O(7)#5	1.931(17)	2.772(2)	165(2)
O(10)−H(7B)···O(6)#6	1.772(16)	2.629(2)	170(2)

[a] Symmetry transformations used to generate equivalent atoms: #1 $x-1, y, z$; #2 $x+1, y-1, z$; #3 $-x, -y+1, -z$; #4 $-x+1, -y+1, -z$; #5 $-x+2, -y, -z+1$; #6 $-x+1, -y, -z+1$.

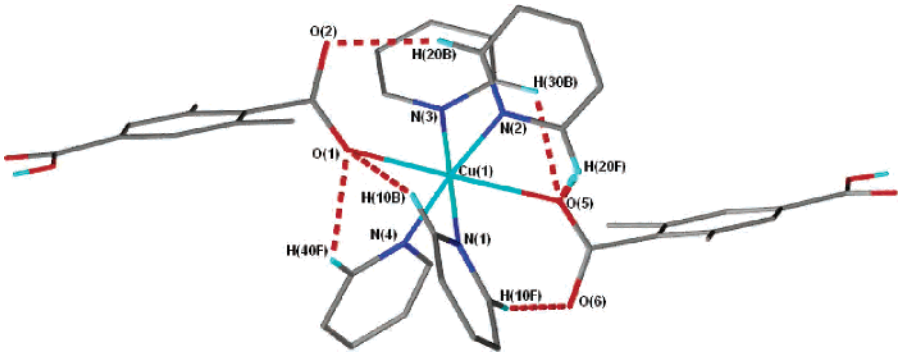

Figure 11. [C−H···O] Bonds in **6**. Phenyl groups, water, and non-hydrogen bonded hydrogens have been removed for clarity.

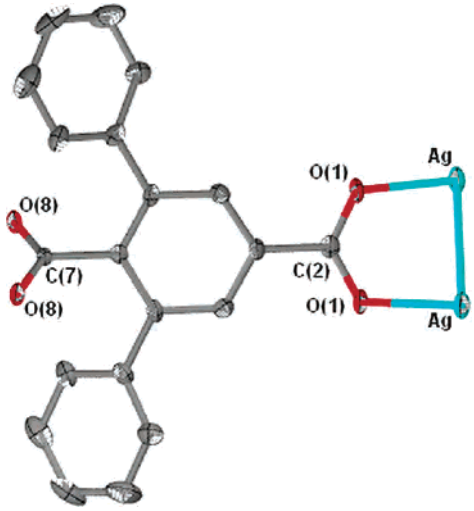

Figure 12. Structure of **7**. Thermal ellipsoids are shown at 50% probability, and all hydrogen atoms have been removed for clarity.

tween the pocket carboxylate and the ortho hydrogens of the coordinated pyridines (Figure 11). The free pocket oxygens each form a single short [C−H···O] bond of 2.332 and 2.292 Å for O(2) and O(6), respectively. The two copper-coordinated oxygen atoms each engage in two [C−H···O] bonds, ranging from 2.413 to 2.522 Å. This results in two pyridines using both ortho hydrogens to interact with opposite carboxylates and two pyrdines using only a single ortho hydrogen atom.

In compounds **3**−**6**, the coordinated pyridine molecules are occupying at least two metal coordination sites, limiting the dimensionality of the resulting complex. In an attempt to prepare a pyridine-free complex based solely on metal−ligand interactions rather than hydrogen-bonding, silver nitrate was reacted with the dipotassium salt of **1** in methanol and water. The resulting 2-D network, **7**, is the only one in this series to be free of both solvent and base, with a formula of **1**·Ag_2. The X-ray crystal structure (Figure 12) shows that there is a plane of symmetry down the center of the molecule, similar to that seen in $\mathbf{1H_2}$.

The para carboxylate bridges two silver atoms, with an Ag−O bond length of 2.178(3) Å, and there is also an argentophilic Ag−Ag bond of 2.8689(7) Å. This compares well with the Ag−Ag bond length in metallic silver of 2.889 Å and is at the very low end of the range of silver−silver interactions in coordination networks reported recently.[29]

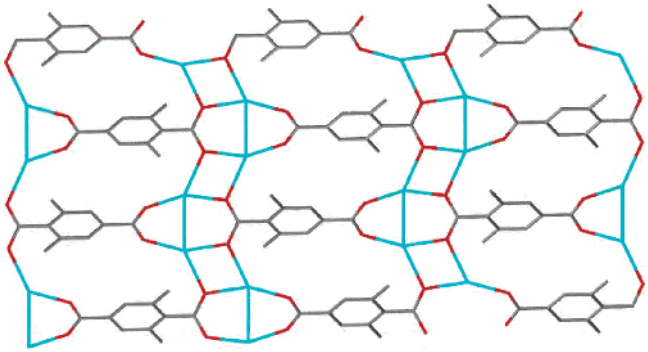

Figure 13. Extended structure of **7**, showing the network formed by Ag−Ag bonds and bridging carboxylates. Phenyl substituents have been omitted for clarity.

Examination of the extended structure (Figure 13) shows that the silver atoms are also coordinated to the pocket carboxylate at an Ag−O bond length of 2.242(3) Å, forming a twisted eight-membered $Ag_2C_2O_4$ ring. Each oxygen of the pocket also bridges a silver from a neighboring chain, Ag−O = 2.430(3) Å, forming a planar four-membered Ag_2O_2 heterocycle.

The *m*-terphenyl ligands are arranged so that the phenyl substituents lie above and below the plane of the 2-D sheetlike network. This allows the phenyls to engage in face-to-face π stacks with the layers above and below (Figure 14). The interaction, which has a centroid···centroid distance of 3.823 Å, is longer than benzene−benzene stacks (3.77 Å),[22] but in the absence of other interactions, the shear number of them surely contributed substantially to the overall stability of the network.

Finally, in another attempt to prepare a low-coordinate, pyridine-free network, $\mathbf{1H_2}$ was combined with zinc nitrate in ethanol. Triethylamine was chosen as the deprotonating agent because of its poor metal-coordination properties compared to pyridine. The base was allowed to slowly diffuse into the reaction mixture as a vapor, leading to the formation of **8** (Figure 15), with a formula of **1**·**Zn**·$\mathbf{(EtOH)_2}$. Both ends of the bifunctional ligand were deprotonated, and two molecules of solvent were incorporated into the structure.

(29) (a) Shorrock, C. J.; Xue, B.-Y.; Kim, P. B.; Batchelor, R. J.; Patrick, B. O.; Leznoff, D. B. *Inorg. Chem.* **2002**, *41*, 6743−6753. (b) Braga, D.; Curzi, M.; Grepioni, F.; Polito, M. *Chem. Commun.* **2005**, 2915−2917. (c) Sun, D.; Cao, R.; Bi, W.; Weng, J.; Hong, M.; Liang, Y. *Inorg. Chim. Acta* **2004**, *357*, 991−1001. (d) Riley, P. J.; Reid, J. L.; Côté, A. P.; Shimizu, G. K. H. *Can. J. Chem.* **2002**, *80*, 1584−1591.

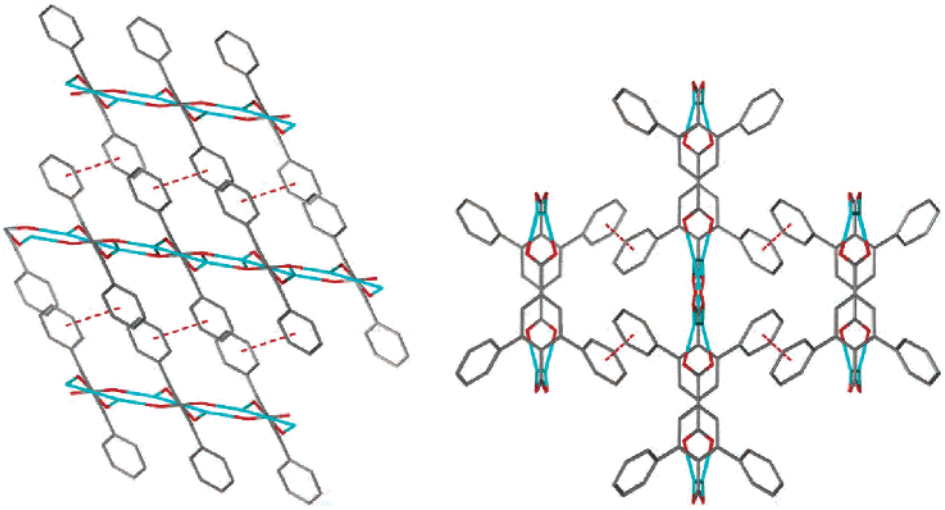

Figure 14. π-Stacking interactions in **7** viewed along the crystallographic *b* and *c* axes, respectively.

Table 4. Selected Bond Lengths (Å) of **8**[a]

Zn(1)−O(41) = 1.926(4)	Zn(2)−O(22)#2 = 1.943(4)	O(201)−H(20A)···O(401)= 2.60(1)	O(401)−H(40A)···O(12)#1 = 2.698(9)
Zn(1)−O(42)#1 = 1.936(4)	Zn(2)−O(21)#3 = 1.953(4)	O(301)−H(30A)···O(601) = 2.58(1)	O(501)−H(50A)···O(52)#5 = 2.79(1)
Zn(1)−O(11) = 1.973(4)	Zn(2)−O(51) = 1.958(4)	O(301)−H(30A)···O(501) = 2.64(1)	O(601)−H(60A)···O(301) = 2.58(1)
Zn(1)−O(201) = 2.008(4)	Zn(2)−O(301) = 1.980(5)		

[a] Symmetry transformations used to generate equivalent atoms: #1 $-x, -y, -z + 3$; #2 $-x, -y, -z + 2$; #3 $x + 1, y + 1, z$; #4 $x - 1, y - 1, z$; #5 $-x + 1, -y + 1, -z + 2$.

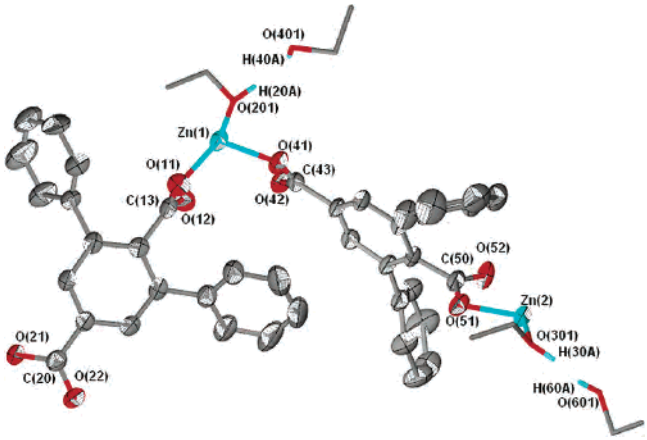

Figure 15. Structure of **8**. Thermal ellipsoids are shown at 50% probability, and all hydrogen atoms except O−H have been removed for clarity. All ethanol molecules are shown as stick drawings, and one of two disordered ethanol molecules has been omitted.

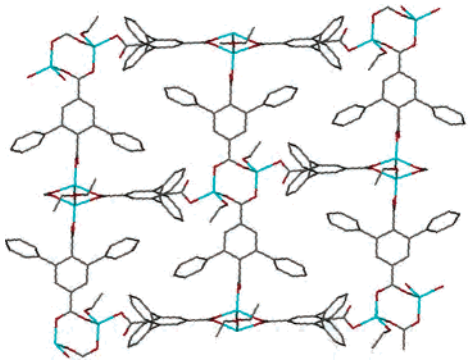

Figure 16. Rectangular grid formed by **8**.

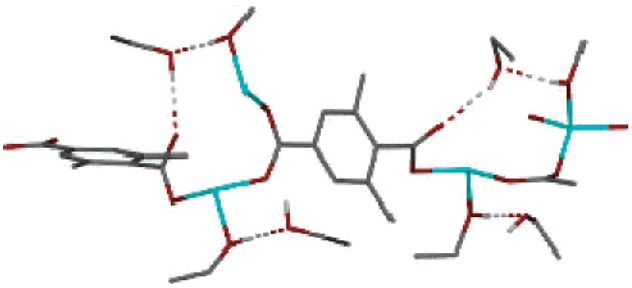

Figure 17. Hydrogen bonding to ethanol in **8**.

The X-ray structure shows two crystallographically distinct molecules in the ASU. The para carboxylates bridge two symmetry-related zinc atoms to form an eight-membered $Zn_2C_2O_4$ heterocycle which makes up the corner of each repeat unit in the rectangular 2-D network of the extended structure (Figure 16). The zinc ions are further coordinated to one oxygen from the pocket carboxylate and one ethanolic oxygen (Table 4).

For each zinc ion, there is also a second equivalent of ethanol that is held in place by hydrogen bonds to the metal-bound ethanol and the extra pocket-carboxylate oxygen (Figure 17). Both molecules of ethanol are intercalated into the space between the layers of the 2-D network, suggesting that they could be removed without affecting the structural integrity of the MOF. Thermogravimetic analysis[15] (TGA) showed a 20% weight loss, corresponding to two molecules of ethanol, up to 225 °C with no further drop until 350 °C when the framework presumably decomposed. Powder diffraction studies of the desolvated network indicated that, while there was still long-range order, the material was no longer crystalline.

Conclusion

A series of MOFs based on the bifunctional *m*-terphenyl ligand $\mathbf{1H_2}$ have been prepared and show a variety of

coordination modes. This sterically demanding ligand has shielded the metal sites from aggregation and network interdigitation, while still allowing for small molecules (pyridine or solvent) to coordinate. This bodes well for eventual applications in gas sorption and/or catalysis. In most cases presented here, hydrogen-bonding or other supramolecular interactions play an important role in determining the overall topology of the networks or chains. The choice of base, solvent, and reaction stoichiometry also influence product formation, but the structures are for the most part dominated by the bulky *m*-terphenyl ligand that effectively limits the dimensionality of the MOFs to two.

Acknowledgment. Funding for this research was provided by the Natural Sciences and Engineering Research Council of Canada (NSERC), Simon Fraser University, Saint Mary's University, the University of Western Ontario, and the Saskatchewan Structural Sciences Centre at the University of Saskatchewan. We thank M. Tracey (SFU) for NMR spectroscopy and M. Yang (SFU) for elemental analyses.

Supporting Information Available: X-ray crystallographic data in CIF format for **2**−**7**; a table of twist angles for **1**−**8**; and powder diffraction data. This material is available free of charge via the Internet at http://pubs.acs.org.

IC051690G